THE CHARACTERISTICS OF A LABORATORY PRODUCED TURBULENT EKMAN LAYER

G. C. HOWROYD and P. R. SLAWSON
Dept. of Mechanical Engineering, University of Waterloo, Waterloo, Ontario, Canada

(Received 7 November, 1974)

Abstract. The characteristics of the atmospheric turbulent Ekman boundary layer have been qualitatively simulated in an annular rotating wind tunnel.

Observed velocity spirals found to exist within the wind tunnel resembled qualitatively those found in the atmosphere in that a two-layer structure was evident, consisting of a log-linear portion topped by an outer spiral layer. The magnitude of the friction velocity u_* obtained from the log-linear profile agreed with that measured directly, i.e., that obtained from the relation: $u_* = (\overline{u'w'})^{1/2}$. Also, the effects of surface roughness on the characteristics of the boundary layer agreed with expected results. In cases where the parametric behaviour predicted by theory departed from the observed behaviour, the probable cause was the inherent size limitations of the wind tunnel. The ability to maintain dynamic similarity is constrained by the limited radius of curvature of the wind tunnel.

The vertical distribution of turbulent intensity in the wind tunnel was found to agree qualitatively with an observed atmospheric distribution. Also, a vertical distribution of eddy diffusivity was calculated from tunnel data and found to give qualitatively what one might expect in the atmosphere.

1. Introduction

The turbulent atmospheric Ekman or spiral layer is characteristically different from the conventional boundary layer as found in flow over a flat plate, in that its thickness remains constant. Within this layer (the layer of frictional influence) the velocity vector changes in magnitude and direction with increasing elevation from the surface.

To date, the dynamics of Ekman layers has been the subject of extensive theoretical but limited experimental study. A few laboratory experimental studies have been conducted in both laminar and turbulent flow (Lilly, 1966; Faller, 1963; Faller and Kaylor, 1966; Faller and Mooney, 1971). Some full-scale studies of the atmospheric Ekman layer have been made such as the Leipzig and Scilly wind profiles (Lettau, 1950; Sheppard *et al.*, 1952). The primary reason for the lack of experimental evidence on the structure of the atmospheric Ekman layer has been in the inherent difficulties involved in acquiring suitable data. By far the greatest experimental difficulty found in the atmosphere is the variability of conditions on a scale of motion in the vertical of approximately one kilometre, which results in a lack of repeatability of results.

The more well known theoretical studies (e.g., Sutton, 1953; Ellison, 1956; Lettau, 1962) have all attempted to model the famous Leipzig wind profile and are based on arbitrary assumptions of the height variation of mixing length. In turbulent flow, however, the mixing length itself is a product of a particular flow field and thus any assumed variation with height can, at best, only yield qualitative information.

The physical importance of the atmospheric Ekman layer is becoming more and

Boundary-Layer Meteorology **8** (1975) 201–219.

more evident, particularly with the advent of the newer industrial 'super stacks' which release their buoyant emissions well within the layer. These emissions are transported by the flow in the layer, the trajectory and rate of spread being affected by the velocity variations both along and across the geostrophic flow component; hence, we might have lateral shear-induced diffusion as another important variable to consider in plume rise and diffusion theory. Also, the ability to predict the height of the layer and the direction of the geostrophic flow component can be useful in weather forecasting applications.

In this paper we shall describe a laboratory wind tunnel designed to simulate the planetary boundary layer consisting of a surface layer (near-constant shear stress) and a turbulent Ekman layer (friction layer).

2. Theoretical Considerations

In order to describe adequately the wind vector variation with height within the planetary boundary layer, one must make some specification of the turbulence structure within the layer as well as impose realistic boundary conditions at the surface and the top of the layer. The turbulence structure has been most often specified through the turbulent exchange coefficients or eddy diffusivities of momentum.

A rather complete theory for the wind distribution was offered by Rossby and Montgomery (1935). These authors chose a two-layer model used earlier by Rossby (1932) and were reasonably successful in predicting the wind speed and direction from a knowledge of surface roughness. In this analysis, the turbulent structure of the flow was described by an eddy diffusivity for momentum K_m; the layer height H and surface shear stress τ_0 were related by;

$$\tau_0 = \varrho f^2 H^2 (9(0.065)^2), \tag{1}$$

where $f = 2\Omega \sin\phi$ is the Coriolis parameter with Ω and ϕ being the angular speed of the earth and the geographic latitude, respectively, and ϱ the air density. By defining a friction velocity u_* as:

$$u_* = \sqrt{\tau_0/\varrho}, \tag{2}$$

Equation (1) becomes

$$H = 0.195\, u_*/f. \tag{3}$$

This relationship was found to agree fairly well with the observed boundary-layer height of the Leipzig profile where the top of the layer was assumed to occur when the wind vector remained constant in direction.

Blackadar (1962) assumed the eddy diffusivity for momentum K_m, to be related to the wind shear by;

$$K_m = \varepsilon^{1/3} l^{4/3} \tag{4}$$

after Heisenberg (1948), where l is the mixing length and ε is the rate of dissipation of turbulent energy per unit mass and may be given by;

$$\begin{aligned}\varepsilon &= K_m \{(\mathrm{d}u/\mathrm{d}z)^2 + (\mathrm{d}v/\mathrm{d}z)^2\} \\ &= K_m s^2,\end{aligned} \tag{5}$$

where u and v are components of the geostrophic wind vector and s is the wind shear. Thus,

$$K_m = l^2 s \tag{6}$$

which is the same relation used by Prandtl (1932) to explain the wind distribution close to the ground. To solve the equations of motion, Blackadar made use of a mixing-length distribution with height found by Lettau (1950) in his analysis of the Leipzig wind profile. The equation which best describes this distribution is given by:

$$l = kz/(1 + kz/\lambda), \tag{7}$$

where k is the von Kármán constant and z is the altitude above ground. The symbol $\lambda = 0.00027\ V_g/f$ is an experimentally determined constant where V_g is the magnitude of the geostrophic velocity. Equation (7) indicates that $l = kz$ for small z (near the ground) and $l = \text{const}$ for large z (near the top of the layer). The height of the Ekman layer in this analysis was found to be;

$$\log_{10} H = 0.008 \log_{10} z_0 + 0.992 \log_{10} (V_g/f) - 2.186, \tag{8}$$

where z_0 is the surface roughness height. In this expression, the second term on the right-hand side is typically much greater than the other two and thus (8) simplifies to:

$$H = \text{const}\ V_g/f. \tag{9}$$

If V_g were replaced by u_* as the characteristic velocity in (9), then an expression similar to that found by Rossby and Montgomery (1935) results (Equation (3)).

Csanady (1967) used dimensional analysis in conjunction with a boundary-layer similarity hypothesis in an attempt to define the Ekman boundary-layer parameters. The layer depth was found to be

$$H = \text{const}\ u_*/f, \tag{10}$$

which is the same as Equation (3).

More recently, Zilitinkevich (1972) estimated the height of the turbulent Ekman layer based on a constant effective eddy diffusivity given by:

$$K_m = k u_* H. \tag{11}$$

Thus, he found the layer height to be approximated by

$$H \simeq k u_*/f \simeq 0.4\, u_*/f, \tag{12}$$

which is twice as large as the predictions of Rossby and Montgomery (1935) and Csanady (1967).

It is therefore evident that the bulk of the theory presented on atmospheric Ekman boundary layers provides us with the following guidelines.

(1) It appears that the depth of the Ekman layer behaves proportionally to the ratio u_*/f.

(2) The distribution of mixing length and eddy diffusivity with altitude have yet to be established satisfactorally, but $l=kz$ in the surface layer and $l=$const in the spiral layer are often assumed (Blackadar, 1962); K_m has been assumed to have various distributions with height.

Thus, a laboratory simulation of the turbulent planetary boundary layer may at least produce additional insight into the qualitative effects of surface roughness, and the distribution of turbulent flow parameters.

3. Experimental Design

An annular rotating wind tunnel first designed and constructed by Mekinda (1971) (see Figure 1) was modified to produce the turbulent Ekman-layer simulation.

The annular duct was constructed from oak and marine plywood with its floor designed for an inclined angle of 45° (actual inclination 41°) to the horizontal. This

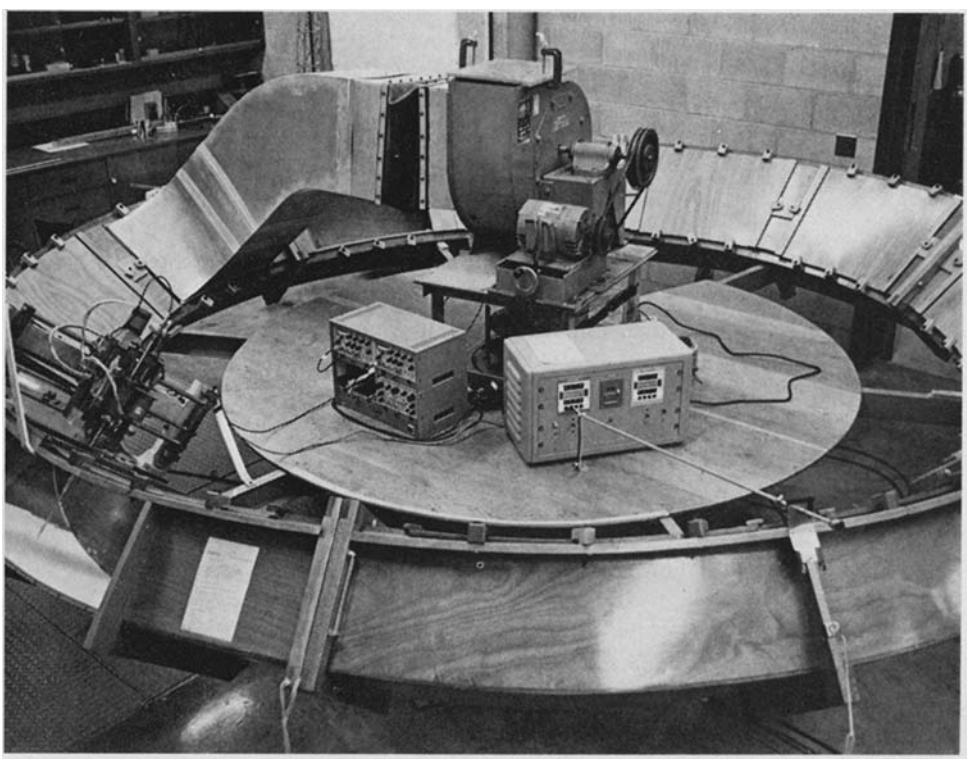

Fig. 1. Photograph of the annular rotating wind tunnel used to simulate the turbulent Ekman boundary layer.

circular wooden duct was in turn fixed to a rigid welded steel frame mounted on a spindle at its centre which allowed the entire assembly to rotate freely. Rotation of the duct was maintained at a constant angular speed by means of a variable-speed direct-current motor located at the base of the structure. Air flow through the duct was supplied by a variable-speed centrifugal fan mounted directly on the rotating platform at the centre of rotation. The fan was mounted in such a way as to draw the air through the duct to avoid fan swirl problems at the inlet. The power to all instrumentation was supplied to the rotating section via a slip ring assembly located at the centre of rotation.

The radius of rotation of the duct was 1.902 m, measured to the centre of the duct cross-section, which measured 45.72 cm wide by 30.48 cm high.

In order to produce an Ekman layer in a wind tunnel of this type, the following criteria must hold:

(1) The flow must be turbulent.

(2) There must be a constant gravitational force which acts perpendicular to the surface.

(3) There must be a force which will only change the direction of the flow and will not increase its energy. This force must increase from the surface up to a point where it is balanced by the pressure gradient force. This force would be analogous to the Coriolis force observed near the Earth's surface.

(4) There should exist dynamic similarity between the atmosphere and the wind tunnel.

From criterion (2) above, the effective gravity $\mathbf{g}_e$ produced at the floor of the rotating duct must be perpendicular to it (i.e., 41° from the vertical). Figure 2 illustrates the force which results in the relation;

$$\cos(41°)\,|\boldsymbol{\omega}^2 R| = |\mathbf{g}|\cos(49°), \tag{13}$$

where $\mathbf{g}$ is the Earth's gravitational force, $\boldsymbol{\omega}$ is the angular velocity of the duct and R is the radius of rotation. Thus, in the absence of streamline curvature, the only force that would act to initiate a deflection of the velocity vector $\mathbf{V}$ would be the Coriolis force $f\mathbf{V}$. However, an order-of-magnitude analysis quickly shows that it is possible that the effects of streamline curvature in this wind tunnel can produce a significant force.

If we consider the duct rotating with an angular speed which satisfies Equation (13), then we find that $\omega = 2.19\ \mathrm{s}^{-1}$ and $f = 2.84\ \mathrm{s}^{-1}$ at the middle of the bottom surface of the duct ($R = 2.0086$ m). The force produced due to the Coriolis force alone based on a free stream velocity of $1.5\ \mathrm{m\ s}^{-1}$ would then be $fV = 4.26\ \mathrm{m\ s}^{-2}$ which acts perpendicular and to the right of the velocity vector in the plane of the duct floor (see Figure 2). At the same time, the force produced due to the rotation of the fluid within the duct itself would then become (after resolving it such that it is perpendicular to $\mathbf{g}_e$),

$$\cos(41°)\ V^2/R = 0.843\ \mathrm{m\ s}^{-2}. \tag{14}$$

The magnitude of this force due to streamline curvature in the duct is about 18% of

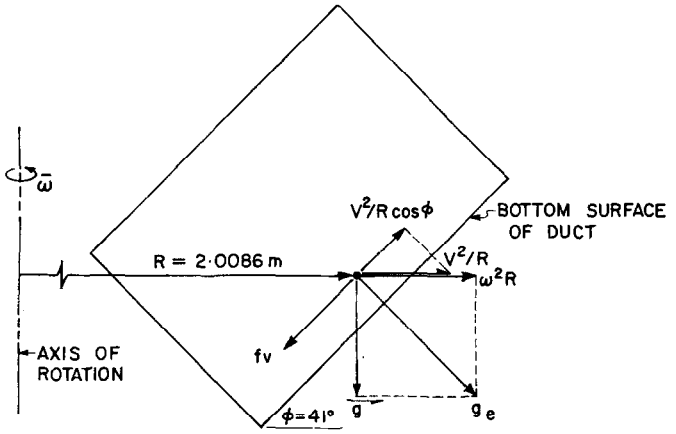

Fig. 2. Force balance showing the forces acting on a parcel of fluid moving through the rotating duct.

the Coriolis force and it acts in the opposite direction. Comparing this value with one found in the atmosphere for a cyclone with a radius of 800 km, a geostrophic velocity V_g of 10 m s^{-1} and a geographic latitude $\phi = 41°$, we find that the Coriolis force $fV_g = 9.53 \times 10^{-4}$ m s^{-2} in the plane of the surface and the force due to cyclone curvature effects would be 1.25×10^{-4} m s^{-2}, which is about 13% of the Coriolis force in magnitude and acting in the opposite direction. Thus we find that the effects of curvature in the wind tunnel for free-stream velocities of 1.5 m s^{-1} or less are not unrealistic although it may be more desirable to eliminate them entirely.

The first criterion for a realistic simulation was that the flow be turbulent. Lilly (1966) has shown that the onset of turbulence in Ekman-layer flows occur at a geostrophic Reynolds number of about 55. In our wind tunnel where $V_g = 1.5$ m s^{-1}, $f = 2.84$ s^{-1} and $\nu = 0.148 \times 10^{-4}$ m^2 s^{-1}, we have

$$\mathrm{Re} = (2V_g^2/\nu f)^{1/2} = 327 \tag{15}$$

which suggests that the flow would be fully turbulent.

It therefore appears that if the free-stream velocity of the air inside the duct is kept to a value below 1.5 m s^{-1} and the tunnel is rotated at a speed which satisfies Equation (13), then a realistic simulation of the Ekman layer should be expected. However, the final criterion for a realistic simulation is that dynamic similarity exists between the atmosphere and the wind tunnel. Csanady (1967) deduced that the dependent variables in the boundary layer (i.e., H, u_* and α, the cross-isobar angle) were functions only of the independent variables (V_g, f, z_0). Further, a non-dimensional grouping of these variables results in:

$$\begin{aligned} u_*/fH &= \beta_1 (V_g/fz_0) \\ u_*/V_g &= \beta_2 (V_g/fz_0) \\ \alpha &= \beta_3 (V_g/fz_0). \end{aligned} \tag{16}$$

Thus for dynamic similarity to exist, the non-dimensional terms on the left-hand side of Equation (16) must be the same in the model as in the atmosphere.

The principal variable of interest in the present study is the velocity vector as a function of altitude above the duct floor for different surface roughnesses. The flow velocity and direction were monitored by using standard DISA/hot-wire anemometry equipment which was mounted directly on the rotating platform as shown in Figure 1.

To determine the velocity and direction of the mean flow, a standard single platinum plated tungsten hot wire was used in all experiments. It was felt that rather than using a conventional 'x' or cross-wire probe, a single wire could be used to produce more reliable results. The probe body was oriented normal to the flow (and to the duct floor, i.e., vertically from the duct floor). The probe body was mounted on a

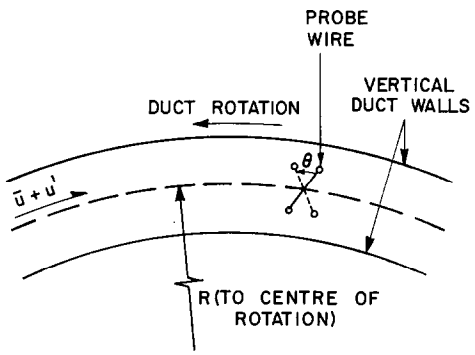

Fig. 3. Schematic Drawing showing the relative rotational motion of the sensing wire.

specially constructed traversing mechanism which could move the hot wire vertically as well as rotate it in a plane parallel to the duct floor (see Figure 3). Movements of the probe wire were made by means of two precision stepping motors with incremental step distances of 0.00025 cm vertically and 0.18 deg rotationally.

In order to determine the velocity and direction of the flow throughout the boundary layer, the hot-wire probe was set at a specified elevation from the duct floor (as close as possible, 0.1 cm say). The wire was then set at some angle to the assumed flow direction. When sampling was ready to begin, the probe wire was rotated at a known constant rate in one direction and then back to the original position. When rotation was complete, the probe was moved vertically to a new elevation and the rotation was resumed. A strip-chart recorder was used to record the probe voltage. A typical voltage record (after the turbulent fluctuations have been filtered out) can be seen schematically in Figure 4. Thus, with the probe wire rotating at a known constant rate and the strip chart moving at a known constant rate, the angle and velocity of the flow can be determined. From Figure 4, the points D and E can easily be seen to be indicative of the magnitude of the maximum velocity. The distances DC and CE can be found and used to find the angle at which the probe is oriented at the point of maximum velocity (this is possible since the angular position of the wire is known at points A, B and C). The process can then be repeated at a new elevation.

The advantages of using a single-wire system rather than a two-wire system are: (1) the error involved in the calibration of the anemometers is minimized since there is only a single wire; (2) the single wire more closely measures flow conditions at a single point than a cross-wire probe due to the distance between the two wires; (3) the angle of inclination of the placement of the wires on a two-wire probe is much more critical than on a single wire; and (4) there is only one signal to transmit from the rotating tunnel to the stationary recording instruments.

The only disadvantage of this system is that it is very time consuming due to the slow rotation rate of the probe.

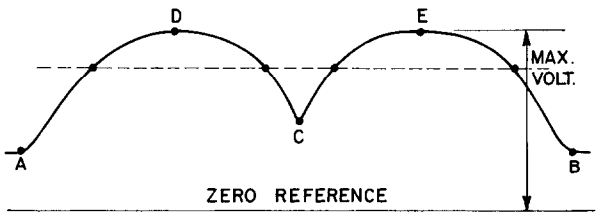

Fig. 4. Schematic representation of a typical probe voltage record.

4. Results

In order to gain a greater insight into the structure of the flow field within the working section of the wind tunnel, contours of the ratio of the mean flow velocity to the maximum value in the lowest 9 cm of the duct cross-section were plotted. These plots were obtained under rotational speeds of twenty RPM (calculation based on radius of rotation 1.95 m) in order to obtain a gravity component perpendicular to the duct floor at the location of interest. These velocity contours are illustrated in Figure 5 for four different surface roughnesses. The surface roughness used along the duct floor for these experiments were: (1) a relatively coarse grained sandpaper; (2) textured paint; (3) bare duct floor coated with clear varnish; and (4) an artificial celanese turf manufactured by Monsanto for use as indoor-outdoor carpeting. This surface had approximately a 0.95-cm knapp.

It is readily noted that all four contours are essentially the same and the general flow structure is relatively unaffected by a change in surface roughness. The only notable change is a slight alteration to the shape and location of the maximum velocity core. The contours show evidence of strong horizontal shearing present to the left of centre of the duct up to at least 9 cm above the duct floor. Beneath the core, however, the isovels appear relatively flat with no evidence of strong horizontal shear. Above the core of maximum velocity, the magnitude of the velocity does not appear to decrease as rapidly as it does below the core which might be construed as providing a useful simulation of geostrophic flow at elevations above the core.

Four distinct sets of experiments were performed in an effort to investigate the effects of surface roughness within the boundary layer along the bottom surface of the duct. The location of interest as determined from the constant velocity contours

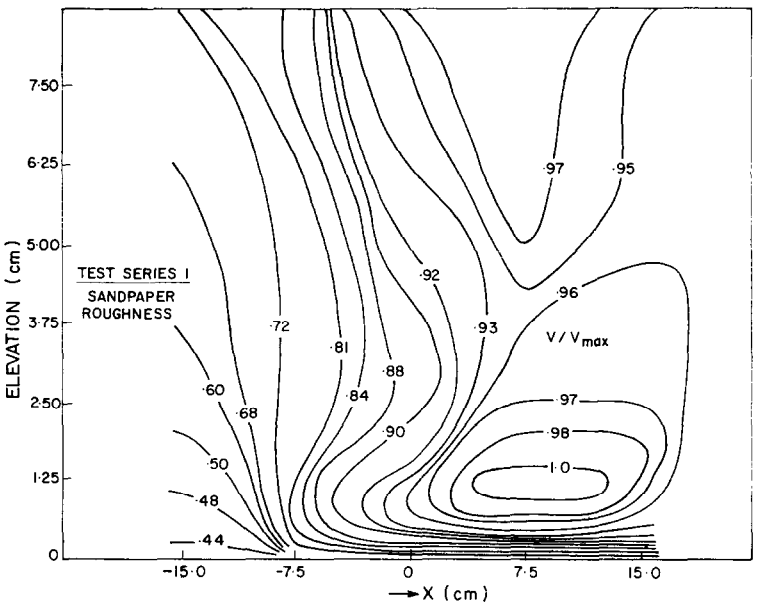
TEST SERIES I
SANDPAPER
ROUGHNESS
V/Vmax
ELEVATION (cm)
7·50
6·25
5·00
3·75
2·50
1·25
0
-15·0
-7·5
0
7·5
15·0
→X (cm)
·97
·95
·92
·96
·72
·81
·93
·88
·60
·84
·68
·90
·97
·98
·50
1·0
·48
·44

Fig. 5A.

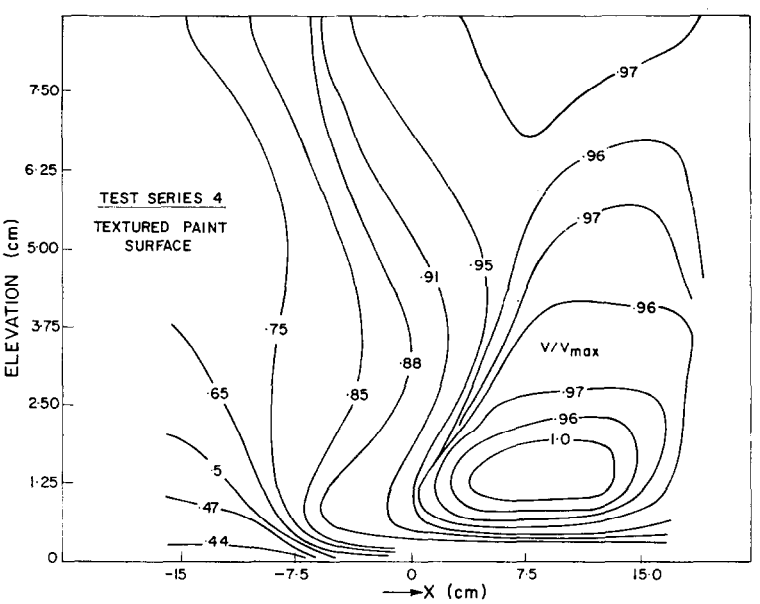
TEST SERIES 4
TEXTURED PAINT
SURFACE
V/Vmax
ELEVATION (cm)
7·50
6·25
5·00
3·75
2·50
1·25
0
-15
-7·5
0
7·5
15·0
→X (cm)
·97
·96
·97
·91
·95
·96
·75
·88
·65
·85
·97
·96
1·0
·5
·47
·44

Fig. 5B.

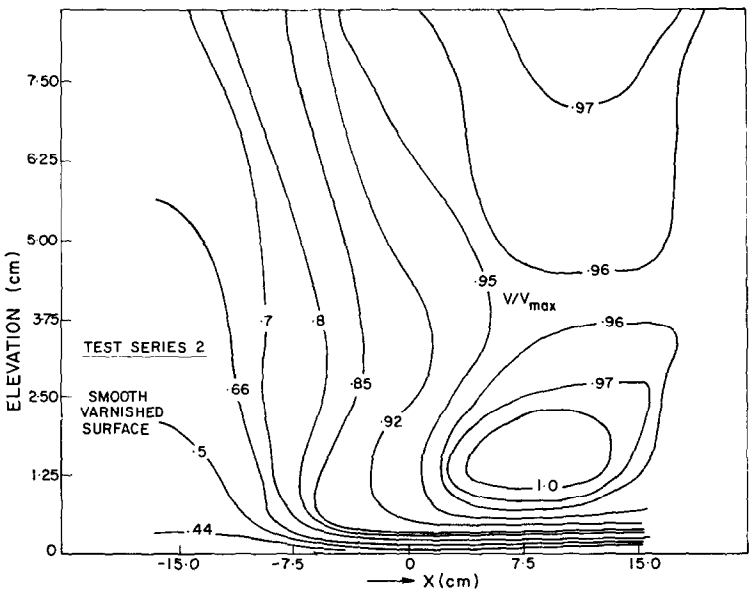

Fig. 5C.

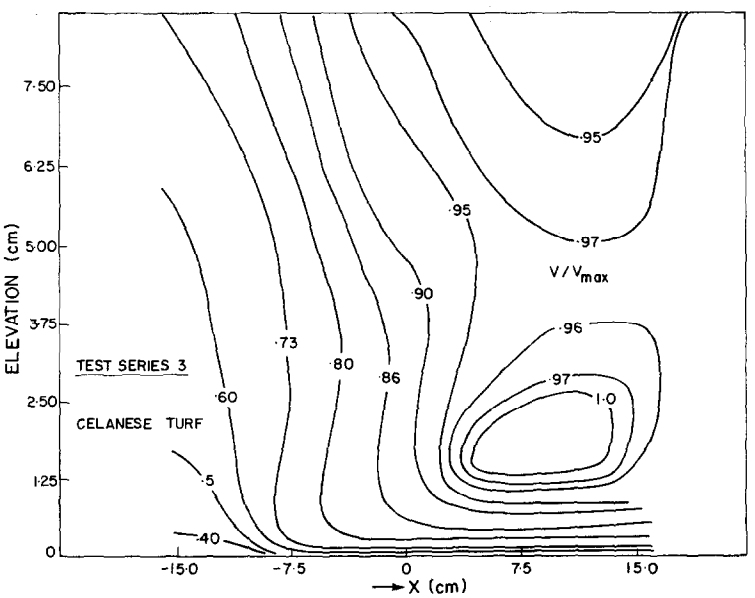

Fig. 5D.

Fig. 5A–D. Non-dimensional constant velocity contours. Cross section is looking downstream.

was 7.5 cm from the centre of the duct floor along the inside radius. For all experiments, the same speed of rotation was used (19.96 RPM) and the mean flow velocity was kept below 1.5 m s^{-1} if possible. Typical velocity spirals as measured within the duct are shown in Figure 6. The observed roughness heights z_0 and friction velocities u_* were determined from the velocity profile itself by fitting the log-linear law in its simplest form,

$$u_* = uk/(\ln z/z_0) \tag{17}$$

to the observed data points (see Figure 7).

The results of all experiments performed over the four surface roughnesses are tabulated in Tables I–IV. Table V contains the average values for all of the observed parameters in Tables I–IV. The height H listed is the observed geostrophic height defined here as the height at which the angular deflection of the velocity vector no longer changes in magnitude. Included in Table V is the standard deviation from the mean value for each of the four series of experiments. From this table one can see

TABLE I

Sandpaper roughness

Expt.	z_0 (cm)	u_* (m s^{-1})	V_{max} (m s^{-1})	Angle (°)	Height (cm)
1.1	0.00393	0.147	1.75	17.5	1.879
1.2	0.00381	0.132	1.57	18.41	2.006
1.3	0.00304	0.114	1.45	18.67	1.820
1.4	0.00330	0.116	1.44	18.15	1.930
1.5	0.00381	0.122	1.52	18.54	1.879
1.6	0.00406	0.122	1.45	17.76	1.879

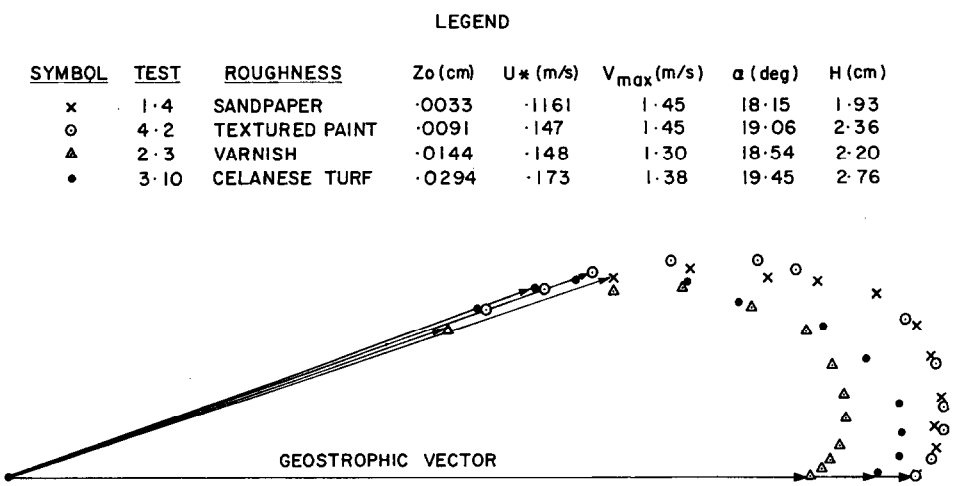

Fig. 6. Wind hodographs over four different surface roughnesses corresponding to rotational speeds of 19.96 rpm ($f = 2.72\ s^{-1}$).

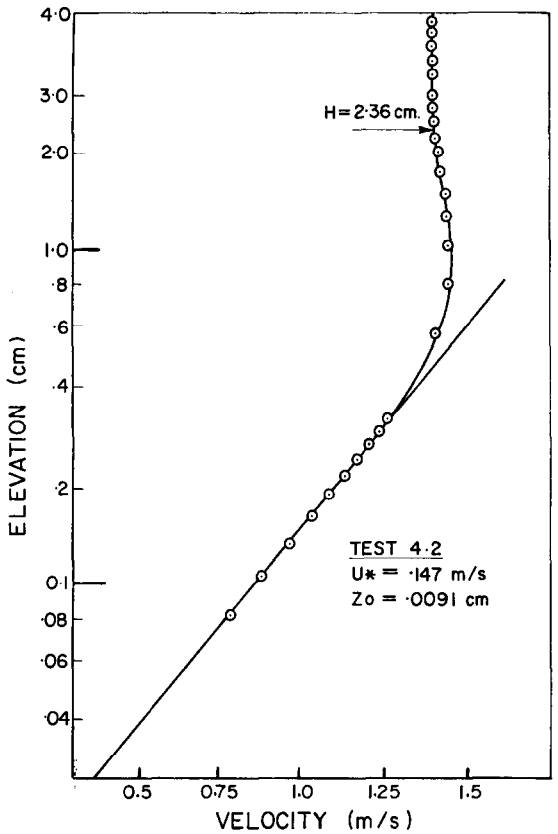

Fig. 7. Typical velocity profile showing the log-linear region of the surface layer from which u_* and z_0 are derived.

that the most unreliable results occurred in the measurements of the angular deflections in test series 3 and 4 since both have a relatively high standard deviation when compared to the difference between the means.

A direct measurement of u_* was made to compare with the results of the above mentioned log-linear method. Standard hot-wire anemometry was used to measure the fluctuating components both along the flow (u') and perpendicularly to the flow (w'), thus giving $u_* = (\overline{u'w'})^{1/2}$. This method resulted in measured values of u_* which agreed closely with those determined by the log-profile method. For example, from test 4.2 the friction velocity determined by fitting a log law in the surface layer was found to be $u_* = 0.147$ m s^{-1}. The value of u_* measured directly was 0.142 m s^{-1}.

There should be a region in the velocity profile where the angular deflection of the velocity vector remains constant (i.e., in the constant stress region) as near the Earth's surface. Some of the spirals in Figure 6 show regions of constant direction while others do not. On this small a scale, however, it is difficult to make many measurements close to the surface. However, this lack of agreement may be attributed

TABLE II

Textured paint surface

Expt.	z_0 (cm)	u^* (m s^{-1})	V_{max} (m s^{-1})	Angle (°)	Height (cm)
4.1	0.008 63	0.147	1.44	19.45	1.993
4.2	0.009 14	0.147	1.45	19.06	2.196
4.3	0.007 87	0.136	1.40	19.45	2.108
4.4	0.008 89	0.141	1.43	19.45	2.133

TABLE III

'Smooth' varnished surface

Expt.	z_0 (cm)	u_* (m s^{-1})	V_{max} (m s^{-1})	Angle (°)	Height (cm)
2.1	0.0132	0.170	1.51	19.32	2.260
2.2	0.0149	0.177	1.50	18.41	2.362
2.3	0.0144	0.147	1.30	18.54	2.209
2.4	0.0147	0.143	1.22	18.41	2.514
2.5	0.0157	0.176	1.50	18.15	2.209
2.6	0.0114	0.151	1.41	21.65	2.438
2.7	0.0109	0.152	1.43	18.41	2.235
2.8	0.0144	0.165	1.42	11.02	2.286
2.9	0.0147	0.164	1.44	16.86	2.438

TABLE IV

Celanese turf

Expt.	z_0 (cm)	u^* (m s^{-1})	V_{max} (m s^{-1})	Angle (°)	Height (cm)
3.1	0.0309	0.205	1.59	12.32	2.750
3.2	0.0266	0.205	1.57	20.36	2.476
3.3	0.0320	0.198	1.50	15.04	2.603
3.4	0.0317	0.193	1.44	13.09	2.730
3.5	0.0279	0.187	1.51	17.76	3.312
3.6	0.0304	0.179	1.38	20.62	3.213
3.7	0.0322	0.195	1.43	17.50	2.933
3.8	0.0271	0.186	1.52	12.97	2.705
3.9	0.0264	0.174	1.43	–	–
3.10	0.0284	0.209	1.75	21.91	2.679
3.11	0.0337	0.201	1.49	17.25	2.832
3.12	0.0309	0.215	1.72	18.28	2.806
3.13	0.0266	0.173	1.42	18.41	2.959
3.14	0.0266	0.179	1.34	17.50	2.806
3.15	0.0266	0.178	1.45	17.12	2.857
3.16	–	–	–	–	–
3.17	0.0266	0.171	1.43	18.67	2.590
3.18	0.0304	0.170	1.36	18.93	2.540
3.19	0.0294	0.173	1.38	19.45	2.768

TABLE V

Average of all test series

Test	$\bar{z}_0$ (cm)	σ_{z_0}	u^* (m s^{-1})	σ_{u*}	$\bar{V}_g$ (m s^{-1})	σ_{v_g}	$\bar{\alpha}$ (deg)	σ_α	H (cm)	σ_H
1	0.00365	0.000383	0.125	0.012	1.53	0.118	18.17	0.46	1.899	0.0508
4	0.00863	0.000533	0.143	0.006	1.43	0.024	19.35	0.02	2.148	0.1524
2	0.01371	0.00165	0.160	0.012	1.42	0.098	18.71	2.86	2.326	0.1117
3	0.02895	0.00241	0.188	0.014	1.48	0.113	17.48	2.72	2.801	0.2184

TABLE VI

Parameter	Atmospheric profile (Leipzig)	Laboratory profile (Test 4.2)
u_* (m s^{-1})	0.502	0.147
α (deg)	26.1	19.06
z_0	0.3 m	0.00914 cm
V_g/u_*	24.24	9.85
f (s^{-1})	1.14×10^{-4}	2.72
H/z_0	3509	258

to two things. Firstly, as the velocity increases with elevation, the effects of curvature and Coriolis force become so great that they initiate a premature deflection of the vector. On the Earth, where the region of constant shear stress is quite thick (50–100 m), the effects of cyclonic curvature and Coriolis force are not as significant as they are in this wind tunnel. Secondly, Tennekes (1972) has shown that the logarithmic velocity profile actually extends beyond the region of constant shear stress. If this is so, then some of the measurements may be in this region.

5. Comparison of the Laboratory Produced Turbulent Ekman Layer with Observation and Theory

Table VI lists the relative magnitudes of various parameters in the turbulent Ekman boundary layer produced in the wind tunnel and in the atmosphere (Leipzig). It is readily seen that the velocity and length scales V_g/u_* and H/z_0 are not similar in model and atmosphere. To approach dynamic similarity one would have to construct a wind tunnel with a radius of approximately 11 m to avoid significant curvature effects (which was not practical). If one were to increase V_g to maintain similarity, a reversal of the velocity vector occurs at a given height above the surface (Mekinda, 1971). Thus, the present tests compromise dynamic similarity to obtain a qualitatively correct velocity distribution.

A comparison between an observed velocity spiral in the wind tunnel with the atmospheric Leipzig profile is illustrated in Figure 8. Both profiles have the same basic shape, with the Leipzig profile having the larger angle of 26.1° while the profile of

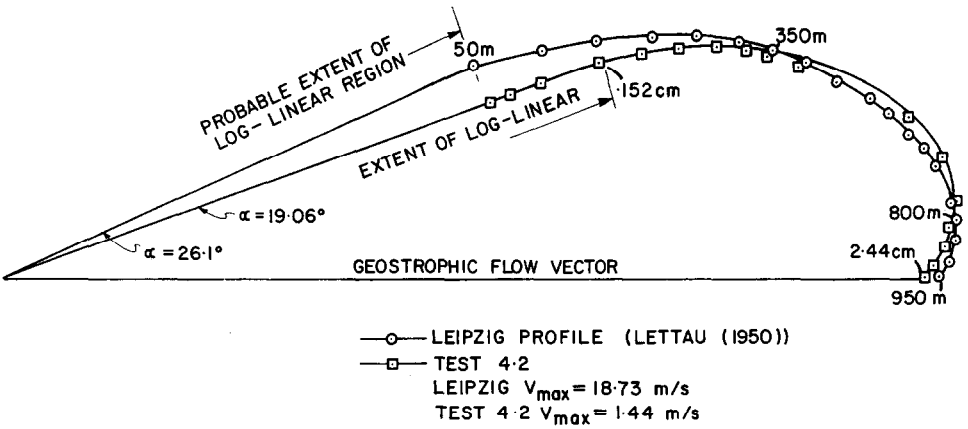

Fig. 8. Non-dimensional wind hodographs (V/V_{max} vs cross-isobar angle) for the Leipzig wind profile (Lettau, 1950) and test 4.2 showing the qualitative similarities in shape and the region of log-law influence.

experiment 4.2 has an angle of 19.05°. If it is assumed that the Leipzig profile is logarithmically linear in velocity up to about 50 m, then both spirals contain log-linear velocity relationships in the same portion of the profile.

Rossby and Montgomery (1935) found that the relation:

$$H = 0.195\, u_*/f \tag{3}$$

agreed well with the observed Leipzig boundary-layer height; however, this formulation yields a considerable underestimate to the heights found in the laboratory work described herein. In Figure 9 one can see that the average observed boundary-layer heights for all experiments agree closely with the relation:

$$H = 0.4\, u_* f \tag{12}$$

found approximately by Zilitinkevich (1972) using similarily theory. This difference may perhaps be attributed to streamline curvature, i.e., the ratios of V_g/u_* cannot be made equal in the model to those in the atmosphere.

The effects of surface roughness on the layer are clearly evident, the rougher the surface, the thicker the boundary layer. Figure 10 represents the geostrophic height as a function of the surface roughness. It is interesting that there is a nearly linear relationship given by:

$$H = 35\, z_0 + 1.778 \text{ (cm)} \tag{18}$$

which indicates a finite boundary layer thickness of 1.778 cm for a 'zero' roughness height. This would of course only hold for a maximum flow velocity within the duct of about 1.46 m s^{-1} (average of all tests). A different relationship should be expected with lower or higher flow velocities since an increased free stream velocity would tend to decrease the boundary-layer thickness and lower free-stream velocities would tend to increase its thickness.

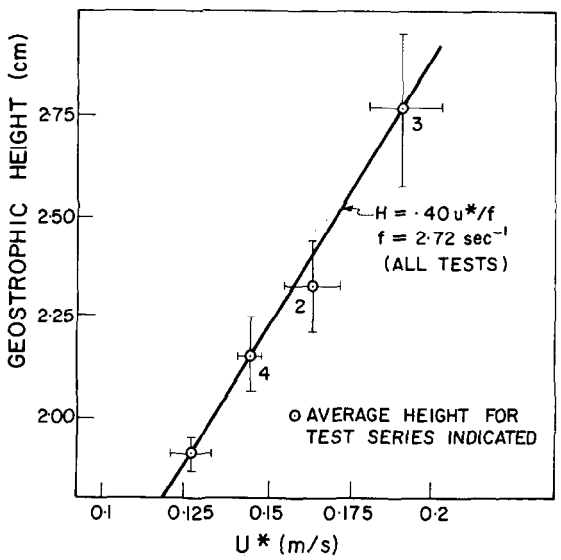

Fig. 9. Observed relationship between geostrophic height H and the friction velocity u^* for all test series.

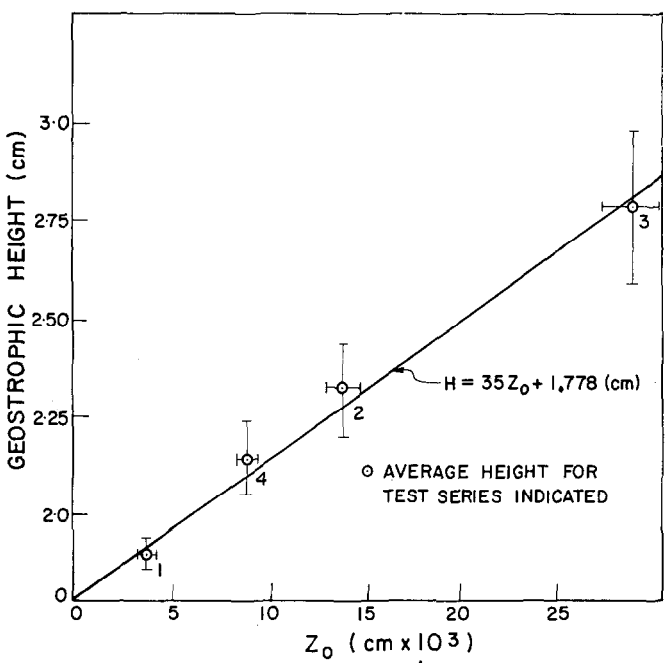

Fig. 10. Observed relationship between geostrophic height H and the surface roughness z_0 for all test series.

In addition to the height and roughness measurements, the turbulence intensity $I=\sigma_V/\bar{V}$, where σ_V is the rms turbulent velocity was measured as a function of altitude above the duct floor and is illustrated in Figure 11. The maximum intensity is located near the top of the surface layer. According to Vinnichenko and Pinus (1973), the variation of turbulent intensity I with altitude in the atmosphere can be approximated by the expression;

$$I = \psi z^{-0.5} \tag{19}$$

based on observed values where ψ is some constant. Figure 11 shows Equation (19) plotted with ψ evaluated as 3.2 which indicates qualitative agreement between observed atmospheric distributions and the laboratory model.

If we now assume that the eddy diffusivity K_m is some function of a turbulent velocity times a length scale then we may write:

$$K_m \simeq I\bar{V}l. \tag{20}$$

Therefore if we use the velocity profile of Figure 7 and the turbulent intensity profile of Figure 11, we can calculate K_m based on an assumed variation of the mixing length l.

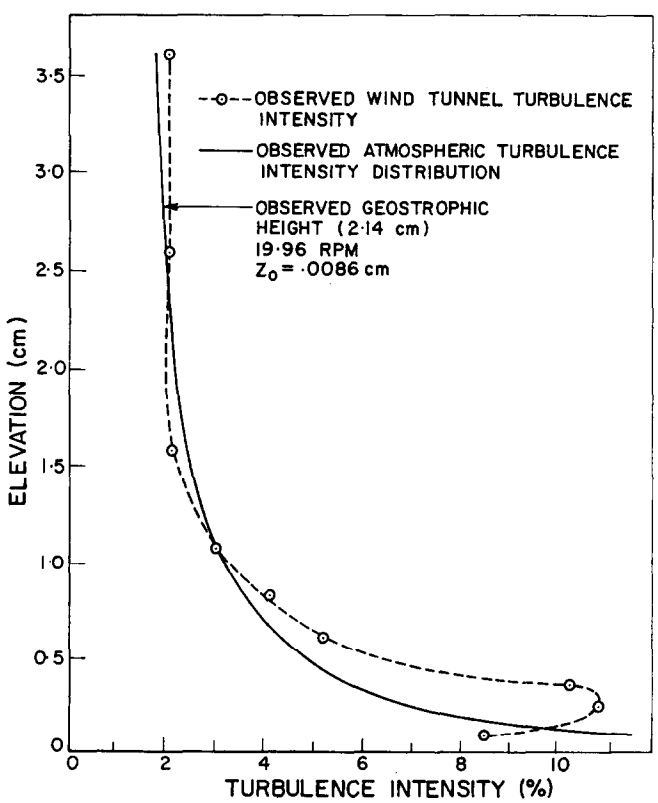

Fig. 11. A comparison between the observed variation of turbulence intensity with height in the simulated and atmospheric boundary layers.

A common mixing-length distribution is given by;

$$\begin{aligned} l &= kz \quad z < h \\ l &= kh \quad z > h \end{aligned} \tag{21}$$

where h is the height of the surface layer (Panofsky and McCormick, 1960; Blackadar, 1962). This results in the vertical distribution for K_m shown in Figure 12 showing an increase to a maximum and decreasing to some constant value as we approach the top of the layer. This type of variation of K_m has been postulated by Blackadar (1962).

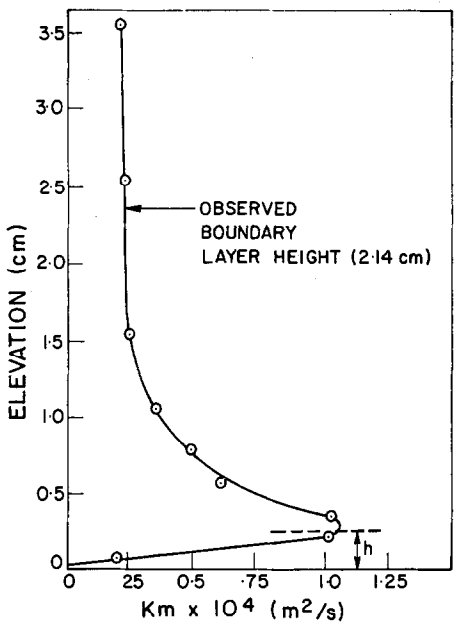

Fig. 12. The calculated variation of eddy diffusivity of momentum with height in the simulated planetary boundary layer.

6. Conclusions

The annular rotating wind tunnel originally designed and built by Mekinda (1971) was modified so that it simulated the turbulent Ekman layer.

Observed Ekman velocity spirals found to exist within the wind tunnel resembled qualitatively those found in the atmosphere. A distinct two-layer structure was invariably observed with a log-type part topped by a spiral outer layer. In the lower part of the log-layer, a constant stress zone was observed in which the velocity direction was essentially constant. This corresponds to the atmospheric surface layer. Friction velocities determined by fitting a log-law to the surface layer compared favorably with those measured directly. The logarithmic region extended above this layer in accordance with atmospheric predictions. When the details of the spirals are compared to those expected from existing theories, variations are evident. Some of

these variations can be attributed to the inherent limitations of the wind tunnel, particularly to the effects of curvature on the airflow induced by the small radius of curvature of the annular duct.

The effects of surface roughness were found to agree qualitatively with observations in the atmosphere. A linear relationship between the geostrophic height H and the friction velocity u_* was found to differ by a factor of two from those predicted by most theories but agreed closely with the approximation of Zilitinkevich (1972).

The vertical distribution of turbulent intensity in the tunnel was also found to agree qualitatively with an observed distribution. A distribution of eddy diffusivity was calculated using the measured turbulent intensities and mean velocities and found to agree qualitatively with the distribution one might expect in the atmosphere. If one were able to construct a large enough wind tunnel of this type, a better agreement between atmospheric observations and the wind tunnel should be expected.

References

Blackadar, A. K.: 1962, 'The Vertical Distribution of Wind and Turbulent Exchange in a Neutral Atmosphere', *J. Geophys. Res.* **67**, 3095–3102.

Csanady, G. T.: 1967, 'On the Resistance Law of a Turbulent Ekman Layer', *J. Atmospheric Sci.*, **24**, 467–471.

Ellison, T. H.: 1956, 'Atmospheric Turbulence', in *Surveys in Mechanics*, Cambridge University Press, 400–430.

Faller, A. J.: 1963, 'An Experimental Study on the Instability of the Laminar Ekman Boundary Layer', *J. Fluid Mech.* **15**, 560–576.

Faller, A. J. and Kaylor, R. E.: 1966, 'A Numerical Study of the Instability of Laminar Ekman Boundary Layer Flow', *J. Atmospheric Sci.* **23**, 466–480.

Faller, A. J. and Mooney, K. A.: 1971, 'The Ekman Boundary Layer Stress Due to Flow over a Regular Array of Hills', *Boundary-Layer Meteorol.* **2**, 83–107.

Heisenberg, W.: 1948, 'Zur statistischen Theorie der Turbulenz', *Z. Physik* **124**, 628–657.

Lettau, H.: 1950, 'A Re-Examination of the "Leipzig Wind Profile"', *Tellus* **2**, 125–129.

Lettau, H.: 1962, 'Theoretical Wind Spirals in the Boundary Layer of a Barotropic Atmosphere', *Beitr. Phys. Atmos.* **35**, 195–212.

Lilly, D. K.: 1966, 'On the Instability of Ekman Boundary Layer Flow', *J. Atmospheric Sci.* **23**, 481–494.

Mekinda, M.: 1971, 'Rotating Wind Tunnel Simulation of the Atmospheric Ekman Boundary Layer', M.A.Sc. Thesis, University of Waterloo.

Panofsky, H. A. and McCormick, R. A.: 1960, 'The Spectrum of Vertical Velocity near the Surface', *Quart. J. Roy. Meteorol. Soc.* **86**, 495–503.

Prandtl, L.: 1932, 'Meteorologische Anwendung der Stromunglehre', *Beitr. Phys. Atmos.* **188**.

Rossby, C. G.: 1932, 'A Generalization of the Theory of the Mixing Length with Application to the Atmospheric and Oceanic Turbulence', *MIT Tech. Papers* **1** (4).

Rossby, C. G. and Montgomery, R. B.: 1935, 'The Layer of Frictional Influence in Wind and Ocean Currents', *MIT Paper Phys. Oceanogr. Met.* **3**, 101 pp.

Sheppard, P. A., Charnock, H., and Francis, J. R. D.: 1952, 'Observations of Westerlies over the Sea', *Quart. J. Roy. Meteorol. Soc.* **78**, 563–582.

Sutton, O. G.: 1953, *Micrometeorology*, New York, McGraw Hill, 327 pp.

Tennekes, H.: 1972, 'The Logarithmic Wind Profile', *J. Atmospheric Sci.* **30**, 234–238.

Vinnichenko, N. K. and Pinus, N. Z.: 1973, in A. MacRonald (ed.), *Turbulence in the free Atmosphere*, Consultants Bureau, New York.

Zilitinkevich, S. S.: 1972, 'On the Determination of the Height of the Ekman Boundary Layer', *Boundary-Layer Meteorol.* **3**, 141–145.